Lawrence Berkeley Laboratory
UNIVERSITY OF CALIFORNIA

ENERGY & ENVIRONMENT
DIVISION

Submitted to Analytical Chemistry

NITRIC OXIDE DETERMINATION UTILIZING A ZEEMAN-TUNED, FREQUENCY-MODULATED ATOMIC LINE SOURCE

Hideaki Koizumi, Tetsuo Hadeishi and Ralph D. McLaughlin

April 1979

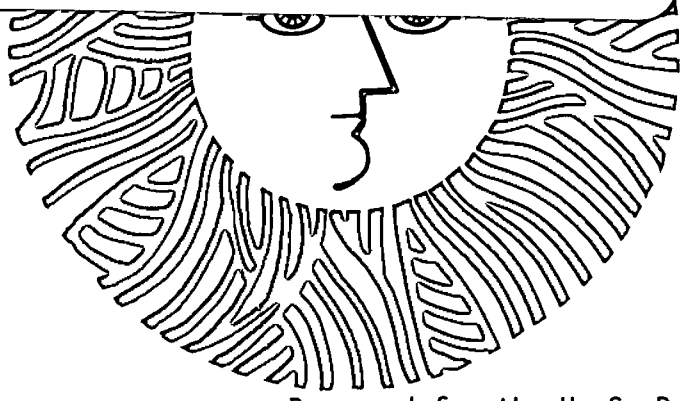

Prepared for the U. S. Department of Energy
under Contract W-7405-ENG-48

DISCLAIMER

NO DETERMINATION UTILIZING A ZEEMAN-TUNED, FREQUENCY-MODULATED ATOMIC LINE SOURCE†

Hideaki Koizumi,* Tetsuo Hadeishi and Ralph D. McLaughlin

Lawrence Berkeley Laboratory, University of California
Berkeley, CA 94720

Abstract

Magnetically tuned emission lines from ions and atoms were utilized to determine concentrations of NO gas with high selectivity and high sensitivity. One of the Zeeman components of an emission line was shifted to exactly coincide with a single rotational-vibrational line of NO, whereas the other component was shifted away from the NO line. The coincident component indicated the extent of NO absorption and the noncoincident component measured the extent of background absorption. By making use of a differential measurement, light scattering and molecular absorption caused by coexisting small particles and gases were cancelled out. Detection limits of NO in N_2 were about 30 ppb and 150 ppb at low pressure and at atmospheric pressure, respectively. The precision is comparable to the detection limit.

*Present address: Naka Works, Hitachi Ltd., Katsuta Ibaraki 312, Japan.

†This work was performed under the auspices of the U.S. Department of Energy under contract no. W-7405-ENG-48.

Introduction

Nitric oxide is a necessary reagent in the photochemical reactions that are responsible for smog formation caused by emission of automobile and plant exhausts, into the ambient air. In situ detection of NO in flames is an important tool for combusion diagnostic research programs that may be important in the control of emissions. Traditionally, the detection of NO has been accomplished by oxidation to NO_2 followed by absorption into a solution containing a colorimetric reagent (1). In addition, infrared absorption spectroscopy has been used. However, these techniques severely suffer from interferences caused by large concentrations of coexistent gases and do not have the capability for in situ measurements or, in the case of infrared spectroscopy, do not have the sensitivity for in situ measurement.

Because of the need for highly sensitive and accurate determinations of NO, several new techniques have been developed. These include Laser Magnetic Resonance using a H_2O far-infrared laser (2)-(4), Zeeman-modulated infrared absorption using a CO laser (5), infrared optoacoustic spectroscopy with a CO laser (6) and UV absorption using a field modulated NO light source (7).

In general, because of the differences in the values of the oscillator strengths for transitions, a measurement that depends on an electronic transition of a molecule will be more sensitive than one that depends on a vibrational rotational transition in the infrared (IR) or far infrared (FIR) spectral region. The sensitivity of photodetectors is also better in the UV region than in the IR region. However, the spectrum due to electronic

vibrational rotational transitions in the UV is much more complicated and less selective than vibrational rotational IR or rotational FIR transitions. In the vast majority of cases, the rotational structures can be resolved in the IR and FIR spectrum, but not in the UV spectrum except for the case of small molecules (8). Even for small molecules, high resolution (~50,000) is required for the observation of rotational structure. Since the sharp structure that is necessary for high specificity is difficult to observe, UV spectroscopy has not been used as frequently as IR spectroscopy for the analysis of contaminants that coexist with other kinds of molecules.

Recently, we have developed a new technique for NO determination by utilizing UV absorption of a magnetically tuned and frequency modulated atomic line source. This method allows high resolution spectra to be obtained without the difficulties associated with the use of a high resolution spectrograph. In this technique, one of the Zeeman components of the emission line is exactly tuned to coincide with a single rotational-vibrational line of NO while the other component is shifted away from the NO line. The matching component indicates the extent of NO plus background absorption and the unmatching component indicates background absorption only. A differential measurement is made of the intensity of these two components. In addition to being highly specific, this technique is capable of high sensitivity because the oscillator strengths of electronic transitions in the UV, VUV and visible regions are much larger than these for vibrational-rotational transitions in the IR and FIR regions. Furthermore, the true absorption coefficients of NO electronic transitions have been shown to be

several hundred times larger than values obtained from low resolution measurements (9). By using an exactly tuned very narrow atomic line, the high sensitivity predicted by the true absorption coefficient can be obtained. It would not be possible to obtain this sensitivity with a continuous source because the light intensity over the small spectral interval of a few GHz is too low. This is the same situation as exists in the field of atomic absorption spectroscopy where neither high sensitivity nor good linearity can be obtained by D_2 and Xe lamps.

In a vast majority of cases, this technique does not suffer from interference because of absorption and light scatterings caused by coexistent large molecules and small particles in the absorption region. This is true because the absorption due to electronic transitions of polyatomic molecules is almost always constant over a spectral region of a few GHz and hence there is no difference in absorption between the two Zeeman components. Reasons why continuous absorption is associated with electronic transitions in polyatomic molecules are discussed by Hertzberg (8). Because of high moments of inertia, predissociation is likely, which results in line broadening. Also, there are many allowed transitions which increases the likelihood of overlap which results in continuous spectra. Even a simple IR spectrum may not predict a simply UV spectrum because the rotational constants may differ greatly between the upper and lower state. Furthermore, even if another molecule in the sample displayed rotational structure, it would be very unlikely that a component magnetically tuned to the NO line would also overlap the rotational line of the other molecule. Since the two components are

equally diminished by Rayleigh and Mie scattering caused by molecules and small particles, no differential signal is produced because of these effects. Therefore, this approach should be very powerful for in situ analysis of NO in samples containing smoke, or a mixture of various kinds of gases.

Experimental Design

Experimental instruments and parameters are listed in Table 1. A block diagram of the system is shown in Figure 1. Figure 2 shows the construction of the light source. This light source is a modification of a magnetically confined arc lamp, described by Hadeishi and Anderson (10). The pole pieces were made of permendur and the chamber of stainless steel. Ar gas flowed through the light source at a pressure of 2-5 torr. The cathode was made of a metal or compound that would yield the desired spectrum. To get Zn spectrum, brass was used. To get Cd ion and atomic spectra, CdO powder was packed in a hole in the cathode (diameter:3mm). When Cd hyperfine structure caused problems, a single isotope (^{114}CdO) was used. The anode was surrounded by an insulator to minimize the likelihood of discharge to the wall. Both D.C. and R.F. power were applied to the light source simultaneously using a circuit described earlier (11). The R.F. power reduced the discharge voltage by a factor of ten, increased the stability of the discharge in the high magnetic field and decreased self absorption. The gas temperature of the discharge was directly measured utilizing a small thermocouple insulated by a thin ceramic coating. The gas temperature depended upon the D.C. power, R.F. power, magnetic field, gas pressure and gas flow rate.

The pole pieces were welded to the discharge chamber (Figure 2). A hole in the magnet through the pole piece and a yoke allowed the radiation to be observed in a direction parallel to the magnetic field. A small condenser lens was placed in the pole piece to increase the amount of light

escaping from the chamber. A new type of half-wavelength plate was developed for this experiment. It consisted of a fused quartz block that was under pressure because of the action of a vise on a strong spring. The applied pressure caused an optoelastic effect and produced a retardation of the phase of the light. The amount of retardation is proportional to the applied pressure. Half wavelength retardation was observed by using crossed polarizers, and quarter wavelength retardation was observed by using a quartz Fresnel rhomb. A linear polarizer was fixed on the shaft of a synchronous motor. Light from a direction parallel to the magnetic field was allowed to pass through a hole made through the shaft of the motor. Then, the right handed and left handed circularly polarized emission from the light source were alternately observed with the rotation of the polarizer.

A differential type pressure gauge was used to accurately measure the pressure in the absorption cell in the pressure range between 0.5 - 110 Torr. High pressure NO and NO-N_2 mixtures were stored in a reservoir made of monel metal. Gases were carried into the absorption cell by evacuating the system.

Results and Discussion

As shown in Figure 3a, NO exhibits sharp γ bands in the UV spectral region. The transition corresponding to the γ bands is $A^2\pi - X^2\Sigma$. The NO γ bands were studied by a number of researchers (12)-(19). Under high resolution, the vibrational lines in Figure 3a exhibit a number of narrow rotational lines, which have also been assigned (12)-(13). Even at N_2 pressures of one atmosphere, the rotational structure of these NO bands appears sharp (14). It is because these rotational lines are so very sharp that it has been difficult to obtain high sensitivity by making a UV absorption measurement using a continuum source. Figure 3a shows the absorption spectrum of NO bands obtained by using a D_2 lamp and a monochromator with a resolving power of 0.1 nm. Figure 3b shows rotational lines in the R_1 branch of the (1,0)(vibrational) transition that are contained in the 214 nm band. These wavelengths were taken from the literature (13) and the intensity was calculated from the Boltzman distribution of the $X^2\Sigma_{1/2}$ ground state at room temperature. The Doppler half intensity width of the individual rotational lines is 2 GHz at 300 K. For NO measurements, one of the Zeeman components of an atomic line is made to coincide with one of the rotational-vibrational lines of NO while the other Zeeman component is shifted away from the rotational-vibrational line.

Accidental near coincidence between rotational-vibrational lines and atomic lines have been used by several researchers to excite a single level of the NO γ bands. Cadmium ion lines at 204.9, 215.1 and 226.5 nm were used to excite (2', 0"), (1', 0") and (0', 0") transitions of NO, respectively (14)-(18). Recently, Melton, et al also reported many atomic line coincidences

in the study of energy transfer in monochromatically excited NO (19). We selected several emission lines to use for the present study. Cadmium ion lines at 214.438 nm and 226.502 nm and a Zn line at 213.856 nm were selected in this experiment because they have simple Zeeman patterns and high intensity. Energy level diagrams for NO showing the transitions that nearly coincide with these ion and atomic lines are shown in Figure 4. v, K and J refer to the vibrational quantum number, rotational quantum number and the vector sum of the rotational and spin quantum numbers, respectively.

Table 2 lists the abundance and the nuclear spin of naturally occurring Cd isotopes. Although the resonance line at 228.8 nm shows only a very small splitting because of the many isotopes, the ion lines at 214.4 and 226.5 nm show a fairly large effect (20). The separation of the components due to the odd isotopes in the 214.4 nm line is 0.519 ± 0.004 cm^{-1} (15.57 ± 0.12 GHz), and in the 226.5 nm line the separation is 0.491 ± 0.007 cm^{-1} ($14.73 \pm$ 021 GHz). To avoid the effects of the hyperfine structure, a single isotope, ^{114}Cd, was used in the basic studies of this technique.

Naturally occurring zinc also contains several isotopes. However, the width of the 213.8 nm line due to hyperfine structure is only about 1 GHz (21). The only isotope with nuclear spin is ^{67}Zn and its abundance is only 4.11%. Therefore, it is not necessary to use a single isotope of Zn in this experiment. Figure 5, which we shall discuss later, shows the relation between the σ^+ and the σ^- Zeeman components and the rotational-vibrational lines of NO. The terms of the upper and the lower states for the atomic lines are listed in Table 3. Only the ^{114}Cd (II) line at 214.6 nm (Figure 5a) has

two σ components of the same circular polarization. The other lines have a single σ component of each circular polarization. As shown in Figure 5, one σ component matching a NO line is used for the measurement of NO absorption while the other component is used to determine the background absorption. In this case, the separation between the σ^+ and the σ^- components is around 2 cm^{-1}(60Gz).

In order to determine the conditions for maximum sensitivity, the magnetic field strength giving the maximum differential absorption between the σ^+ and the σ^- components was measured for the two ion lines and the atomic line.

Figure 6 shows the relation between the strength of the magnetic field applied to the light source and the difference of intensity between the σ^+ and σ^- components for the Cd(II) line at 214.6 nm. A minimum in the curve was observed at a field strength of 5.3 kG because of the presence of two components of the same circular polarization when the single isotope ^{114}Cd was used. When natural Cd was used, the minimum disappeared because the emission line was broadened by the hyperfine structure. A higher sensitivity could be obtained using the single isotope because the emission line is as sharp as the NO absorption line. The highest sensitivity was obtained at 9.2 kG. This measurement was carried out at low pressure so the NO absorption line was very narrow.

Figure 7 shows the relation between the field strength and the intensity of differential absorption for the Zn line at 213.8 nm. There is only one σ component of the same circular polarization in this line. The curve in Figure 7

contains information that would allow the profile of the vibrational rotational NO line to be calculated by correcting for the 1.6 GHz width of the emission line. The highest sensitivity in this case was obtained at the field strength of 20 kG.

These figures also demonstrate the selectivity of this technique. Since the splitting of the Zeeman components is so small, it is highly probable that the background absorption will be constant over this spectral region. If other molecules in the sample show sharp rotational structure it is highly improbable these lines will coincide with the NO line. For the Cd line at 226.5 nm, the maximum differential absorption was obtained at a field strength at 16.5 kG. The magnetic field strengths giving the maximum difference in absorption between the σ^+ and σ^- components for all the lines are listed in Table 3. For routine analysis at near room temperature, the Cd line at 214.4 nm would be the best to use because it does not require high magnetic field. However, for measurement at high temperatures, the Zn line at 213.8 nm should be used because the population of the $J = 29.5$ level as determined by the Boltzmann distribution becomes maximum at 3994°C. In this situation, this line would result in a higher sensitivity than the Cd 214.4 nm line since the population of the $J = 12.5$ level would decrease. Hence, the Zn line should be used for measurement in flames or other combustion systems.

Figure 8 shows the oscilloscope traces of signals from the pre-amplifier (upper traces) and from the synchronous rectifier (lower traces). The natural Cd(II) line at 214.4 nm was used for this experiment. With

this line only one Zeeman component coincides with the NO line of Q=10.5 as shown in Figure 5. As the polarizer rotates first the σ^- component passes through the absorption cell and is absorbed by NO. As the rotation continues the σ^+ component then passes through the absorption cell but is not absorbed by NO. In a vast majority of cases, the intensity of σ^+ and the σ^- components is equally diminished by absorption due to other molecules or by light scattering. It follows that a sine shaped signal is observed if NO exists in the absorption cell. The frequency of this signal will correspond to the frequency of rotation of the motor. The differential absorption between σ^+ and σ^- components results in a output signal from the synchronous rectifier. Since the rotation speed of the polarizer is 3600 r.p.m., the signal can follow rapid changes in NO density and can correct for rapidly changing background absorption. The signal from the synchronous rectifier was recorded on the chart with a time constant of 0.5 sec.

Figure 9 shows one example of NO signals obtained with a 20 cm cell. The lower trace shows the differential absorption between the σ^+ and σ^- components in absorbance units and the upper trace shows the average transmittance of the σ^+ and σ^- components through the cell. In this experiment, the noise level of the base line corresponded to about 4.5×10^{-4} absorbance units. Nitric oxide at the 5 ppm level causes a signal of 0.025 absorbance units. The detection limit is usually defined by the quantity of NO giving rise to a signal twice as large as the noise level. Using this criterion, the lower limit of detection is 180 ppb with the present technique. We also used a 120 cm cell. By putting a lens in the cell, the noise level

was almost the same as that with the 20 cm cell. In this case, the detection limit was about 30 ppb. Higher sensitivity could be obtained by using a long patch cell such as is used in IR spectroscopy because the Cd line can be made very intense.

Figure 10 illustrates the capability of this technique to correct for other molecules in the absorption region. The lower trace shows the differential absorption between the σ^+ and σ^- components in absorbance units and the upper trace the average absorption of the σ^+ and σ^- components in transmittance units. The scale is the same as that of Figure 8. Acetic acid vapor and nitro-benzene vapor were introduced into the absorption cell because both of these compounds have strong absorption bands near the Cd line at 214.4 nm. This indicates that when the absorption from non NO species is as high as 70%, good measurements can still be made.

If oxygen is present, at room temperature, NO will react to form NO_2. Since this compound does not produce a differential absorption signal, it is possible to measure the change of NO concentration when air is introduced into the cell. Figure 11 shows the time dependence of the NO concentration after the introduction of 100 Torr of air. The reaction $2NO + O_2 \rightarrow 2NO_2$ proceeds with a reaction rate proportional to the square of NO concentration, and hence is very slow when the NO concentration is a few ppm (22).

It is difficult to use the fluorescence from NO as a detection method because of quenching by O_2, H_2O, etc. The quenching half pressures of O_2 and H_2O are 1.1 Torr and 0.65 Torr, respectively (23). Hence, NO fluorescence cannot be used to detect NO in the atmosphere. Using the present

Zeeman technique, however, atmosphere measurement is possible.

It was also observed that a surface reaction will rapidly reduce the NO concentration at high temperature when a stainless steel cell is used instead of a quartz cell. The NO concentration rapidly decreased at temperatures about 70°C, even when there was no oxygen in the cell.

Figure 12 shows the time dependent NO signal when 10 Torr of a NO N_2 mixture (NO concentration equals 450 ppm) was introduced into a stainless steel cell.

The NO signal depends upon the pressure of a foreign gas. The emission line width of Cd or Zn is less than 3 GHz, which is determined by the gas temperature of the plasma. The pressure broadening of the emission line is negligibly small because the Ar gas pressure is only a few Torr. The effective cross section for the Lorentz broadening of NO is relatively large. The line width becomes larger than 10 GHz at a foreign gas pressure of 1 atm, whereas it is only 2 GHz at less than 10 Torr at room temperature (24). Therefore, the sensitivity decreases with the foreign gas pressure. Figure 13 shows the relationship between NO absorption and the pressure of N_2. The intensity of NO absorption in N_2 at 1 atm is about one-fourth of that in N_2 at 10 Torr. It was also possible to obtain the pressure dependence of NO absorption when O_2 was the foreign gas. The reaction of NO with O_2 was very slow because the NO concentration was only 20 ppm. The relation between the O_2 pressure and the differential signal was almost the same as that when N_2 was used. Although the signal strength varies with a big change of foreign gas pressure, it should be emphasized that the differential absorption is completely free from the quenching effects that make fluorescent measurements so difficult.

References

(1) A.C. Stern, Ed., "Air Pollution", Vol. 3, Chap. 7, Academic Press, New York, 3rd edition (1976).

(2) M. Mizushima, K.M. Evenson and J.S. Wells, Phys. Rev., A, 5, 2276 (1972).

(3) P.A. Bonczyk, Chem. Phys. Lett., 18, 147 (1973).

(4) S.M. Freund, J.T. Hougen and W.J. Lafferty, Can. J. Phys., 53, 1929 (1975).

(5) A. Kaldor, W.B. Olson, A.G. Maki, Science, 176, 508 (1972).

(6) L.B. Kreuzer and C.K.N. Patel, Science, 173, 45 (1971).

(7) T.T. Kikuchi, Appl. Opt., 13, 239 (1974).

(8) G. Herzberg, "Molecular Spectra and Molecular Structure, II. Spectra of Diatomic Molecules, III. Electronic Spectra and Electronic Structure of Polyatomic Molecules", Van Nostrand Reinhold Co., New York (1966).

(9) H. Okabe, "Photochemistry of Small Molecules", Wiley Inter Science, Somerset, NJ (1978).

(10) T. Hadeishi and T. Anderson, Opt. Com., 23, 252 (1977).

(11) H. Koizumi and K. Yasuda, Spectrochim. Acta, 31B, 237 (1976).

(12) L. Gerö and R. Schmid, Proc. Phys. Soc. London, 60, 533 (1948).

(13) R. Engleman, Jr., P.E. Rouse, H.M. Peek and V.D. Baiamonte, Los Alamos Scientific Laboratory Report LA-4364 (1970).

(14) A.G. Gaydon and A.R. Fairbairn, Proc. Phys. Soc., A67, 474 (1954).

(15) O.R. Wulf: Phys. Rev., 46, 316 (1934).

(16) G.E. Moore, O.R. Wulf and R.M. Badger, J. Chem. Phys., 21, 2091 (1953).

(17) A.B. Kreuhzeps Onmuka U Cnekmpocknie 1, 469 (1956).

(18) H.P. Broida and T. Carrington, J. Chem. Phys., 38. 136 (1963).

(19) L.A. Melton and W. Klemperer, J. Chem. Phys., 59, 1099 (1973).

(20) F.M. Kelly and J.B. Sutherland, Can. J. Phys., 34, 521 (1956).

(21) M.F. Crawford, W.M. Gray, F.M. Kelly and A.L. Schawlow, Can. J. Res., 28, 138 (1950).

(22) J. Heicklen and N. Cohen, "The Role of Nitric Oxide in Photochemistry", Advance in Photochemistry, Vol. 5, p157, Interscience Publishers, New York (1968).

(23) F.P. Schwarz and H. Okabe, Anal. Chem., 47, 703 (1975).

(24) H. Koizumi, T. Hadeishi and R.D. McLaughlin: unpublished work.

TABLE 1. Experimental apparatus and parameters.

Light Source	DC-HF magnetically confined arc lamp (10) (11)
	DC: 50-200V, 50-150mA
	HF: 70 MHz, 10W
	Ar gas pressure: 2-5 Torr, flow rate: 0.1 L/min at 1 atm.
Electromagnet	Varian Associates Model V-4004,
Quarter wave plate	Photoelastic variable retarder
	25 × 12.5 × 12.5 mm suprasil, stress: 0-100 kg
Polarizer	Rochon prism (Ohyokohden Laboratory Co.), artificial
	quartz crystals with optical contact.
Rotator	Hollows shaft synchronous motor, hole diameter: 7 mm
	3600 r.p.m.
Monochromator	J-Y Optical Systems, Model H-20 UV-V, Ap rture
	F:4.2, dispersion: 4nm/mm
Photomultiplier	Hamamatsu TV, R955
Thermometer	Doric Digital Trendicator 400 Type K/°C
	(iron constantan thermocouple)
Log. amplifier	Analog Devices, 755N
Lock-in amplifier	120 Hz Q=25, t=1 sec.
NO gas	Matheson Gas Products Co., Pure NO, 450 ppm NO in N_2, 0.70 ppm NO in N_2, NO_2<0.20 ppm)
Pressure Gauge	Hasting Vacuum Gauge (thermocouple): 10^{-3} to 5 Torr, Wallace and Tiernan Model FA-141 (differential diaphragm gauge): 0.5 to 110 Torr, U.S. Gauge (diaphragm gauge): 25 to 760 Torr
Vacuum pump	The Welch Scientific Co., Duo Seal Vacuum Pump, 17 L/min.

TABLE 2. The isotope abundances for naturally occurring Cd and Zn.

Isotope	Nuclear spin	Abundance (%)
^{106}Cd	0	1.22
^{108}Cd	0	0.88
^{110}Cd	0	12.39
^{111}Cd	1/2	12.75
^{112}Cd	0	24.07
^{113}Cd	1/2	12.26
^{114}Cd	0	28.86
^{116}Cd	0	7.58
^{64}Zn	0	48.89
^{66}Zn	0	27.81
^{67}Zn	5/2	4.11
^{68}Zn	0	18.57
^{70}Zn	0	0.62

TABLE 3. Comparison of atomic lines with near-coincident molecular lines.

Atomic (ion) line	Wavelength (nm)	Transition	Rotational line, J	Observed separation (GHz)	Field strength for matching (kg)
Cd(II)	214.438	$^2S_{1/2}-^2P_{3/2}$	$R_1(12-1/2)$	-12.5	9.2
Cd(II)	226.502	$^2S_{1/2}-^2P_{1/2}$	$Q_2(10-1/2)$	-30.8	16.5
Zn	213.856	$^1S_0-^1P_1$	$Q_1(29-1/2)$	28.0	20.0

Figure Captions

Fig. 1. Block diagram of the experimental apparatus.

Fig. 2. Magnetically confined arc lamp.

Fig. 3. a) Absorption spectrum of NO γ bands 1870 ppm in N_2 1 atm., 10 cm cell.
b) The R_1 branch due to the (1,0) vibrational transition of the NO γ band, at 300K.

Fig. 4. NO energy level diagrams showing those transitions that nearly coincide with the atomic and ion lines used in this study.

Fig. 5. Relationship between the rotational-vibrational line of NO and the Zeeman split atomic line.

Fig. 6. Relation between the magnetic field strength and the differential absorption caused by NO for the Cd(II) line at 214.4 nm.

Fig. 7. Relation between the field strength and the differential absorption caused by NO for the Zn line at 213.9 nm.

Fig. 8. Oscilloscope traces of the signal from the photomultiplier and from the synchronous rectifier.

Fig. 9. NO signal with the present technique. Lower trace: differential signal; upper trace: transmittance of light through the cell.

Fig. 10. Correction for light scattering and absorption by other molecules. Lower trace: differential signal; upper trace: transmission through the cell in absorbance unit.

Fig. 11. Time-dependent NO signal after the introduction of air.

Fig. 12. Reduction of NO signal because of reaction with the walls of a stainless steel cell at high temperature.

Fig. 13. Relation between the differential absorption signal of NO and the pressure of the coexisting N_2 gas.

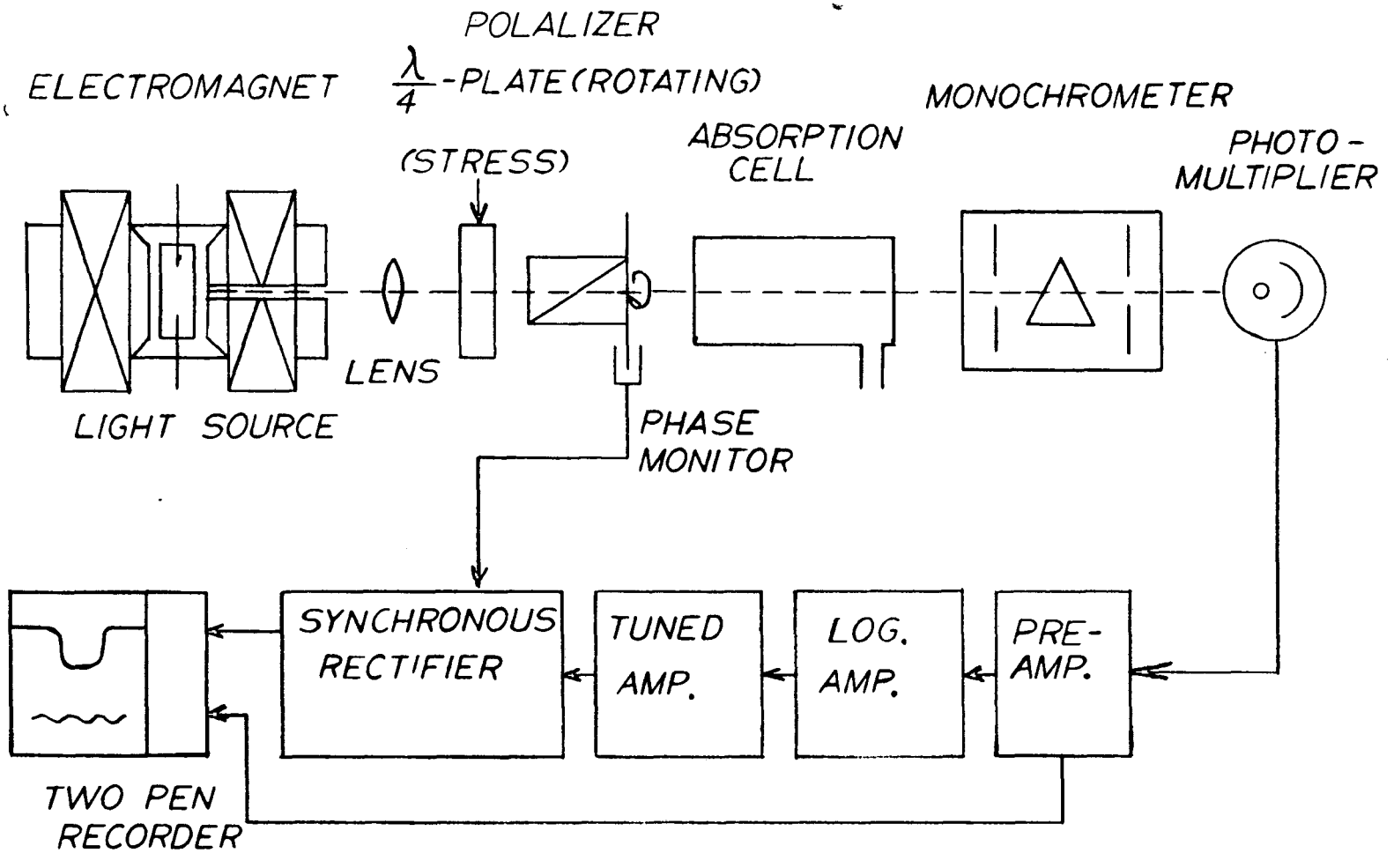

Fig. 1 Block diagram of the experimental apparatus.

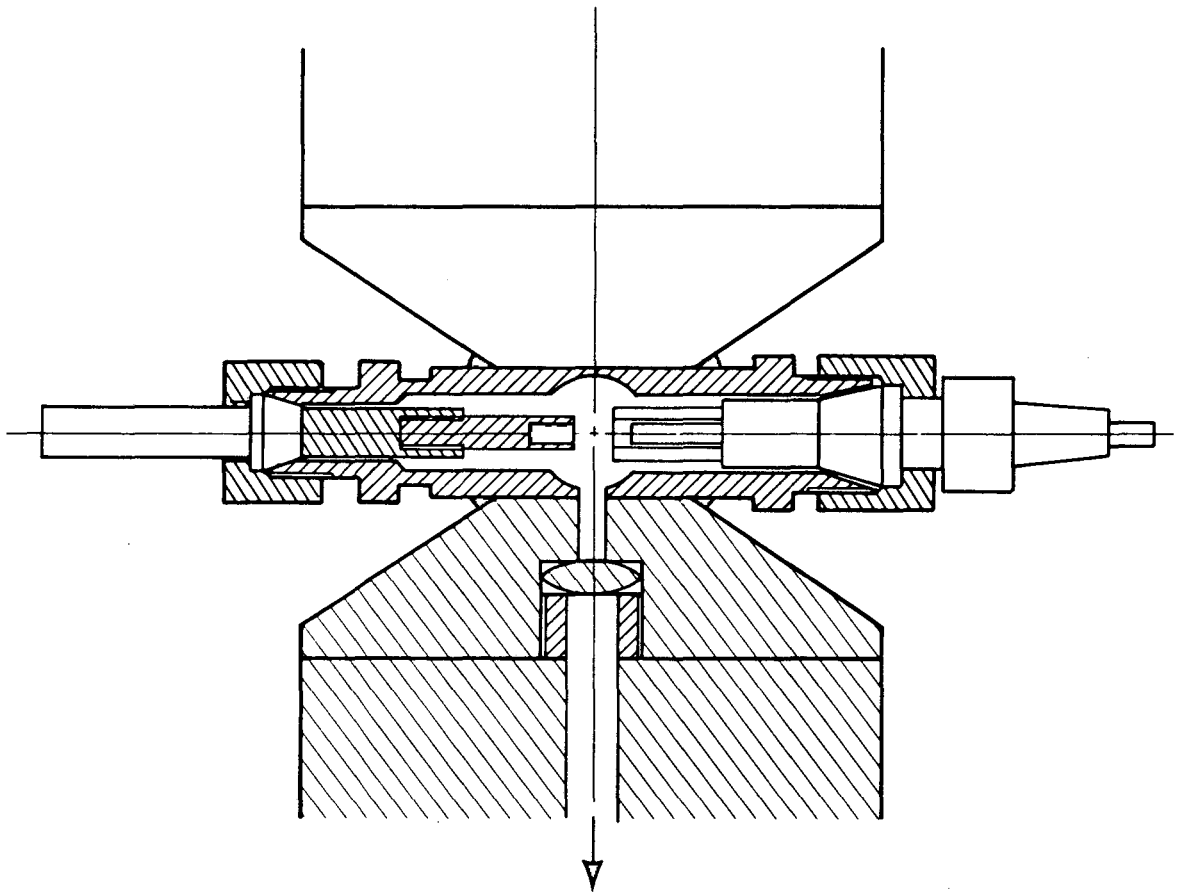

XBL 795-1603A

Fig 2 Magnetically confined arc lamp.

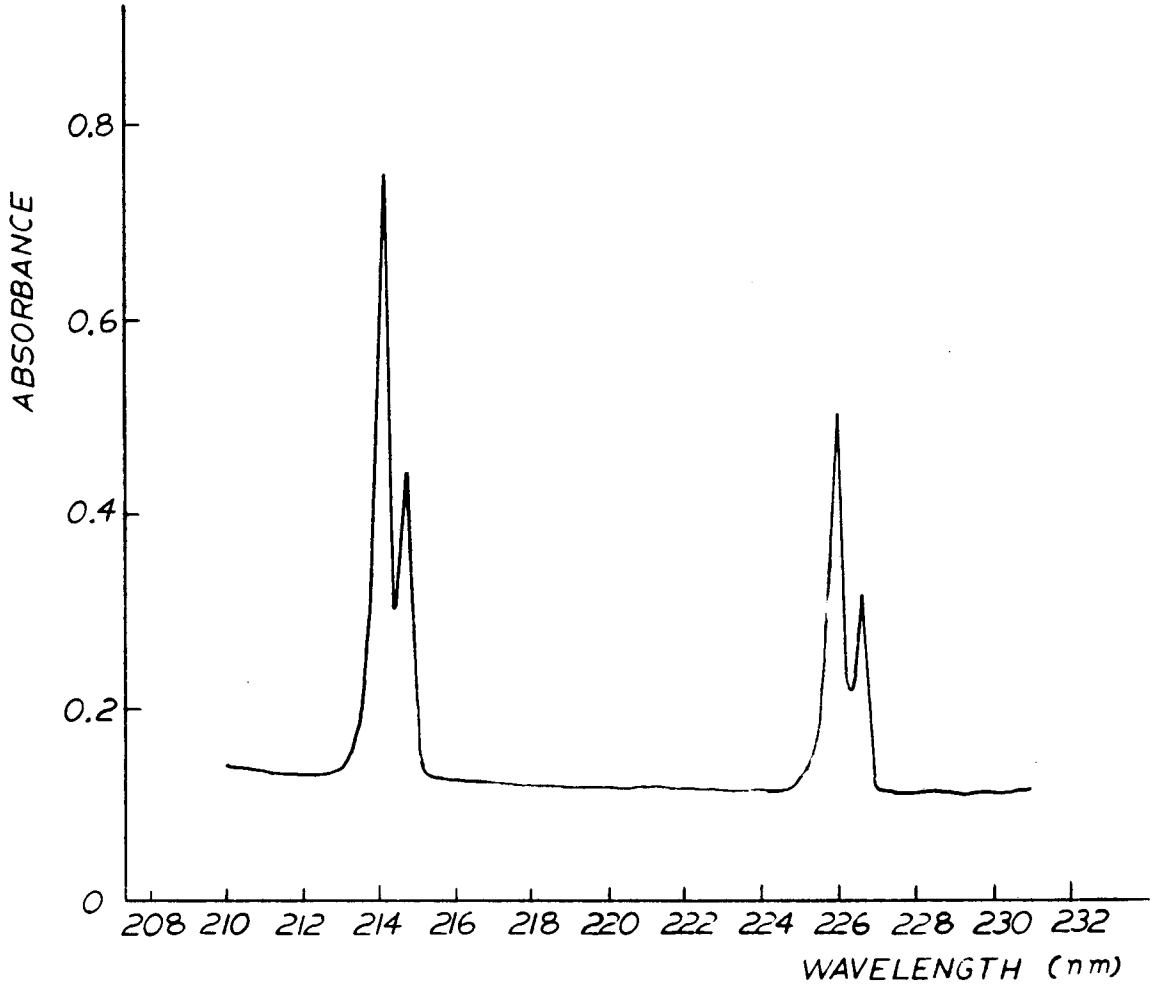

XBL 789-10690

Fig. 3 a) Absorption spectrum of NO γ bands 1870 ppm in N_2 1 atm., 10 cm cell.

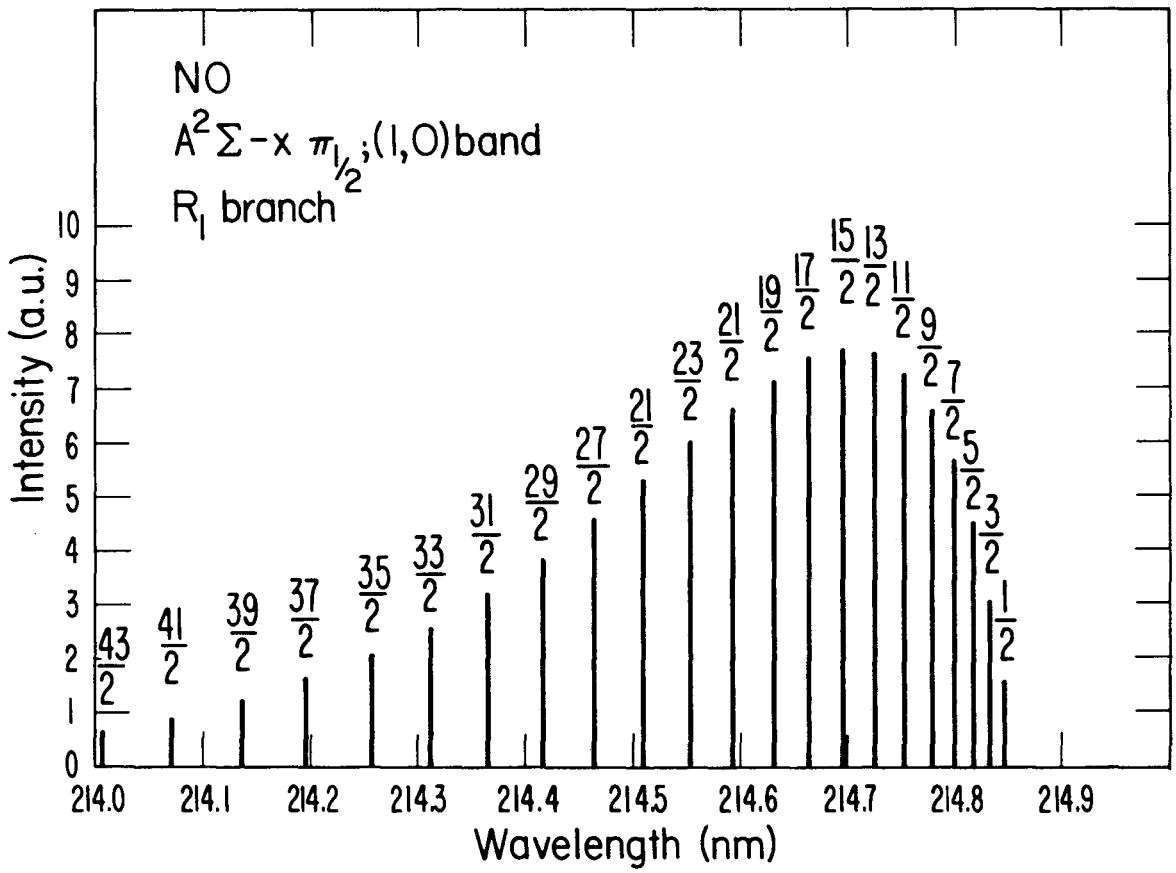

XBL 795-1607

Fig. 3 b) The R_1 branch due to the (1,0) vibrational transition of the NO γ band, at 300K.

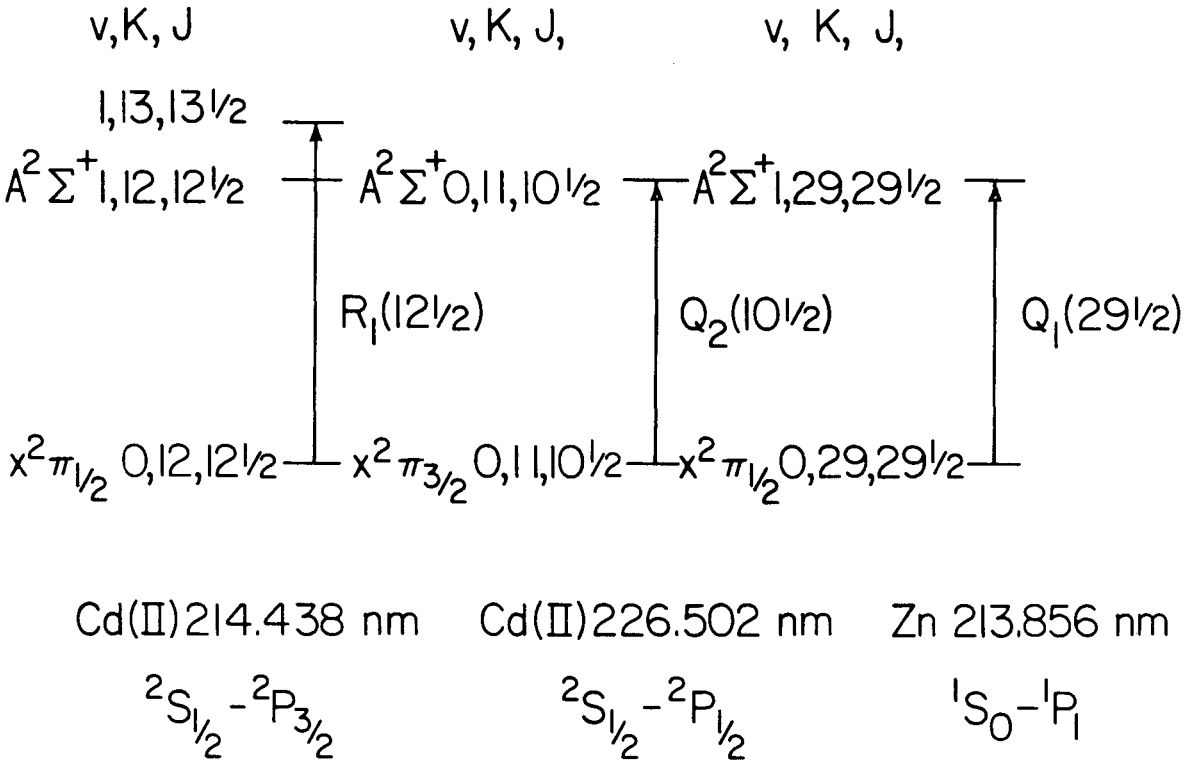

XBL 795-1604

Fig. 4 NO energy level diagrams showing those transitions that nearly coincide with the atomic and ion lines used in this study.

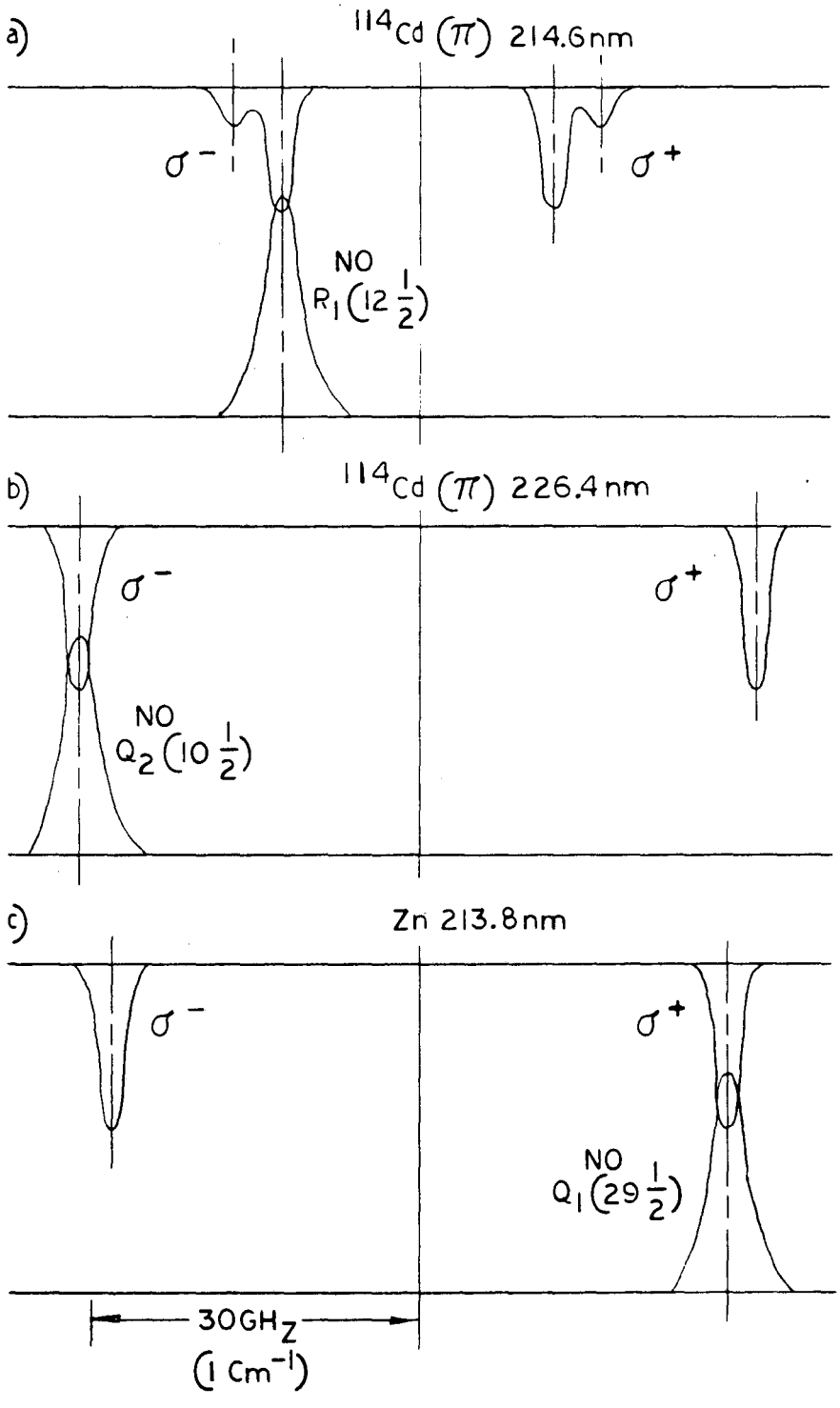

XBL 789-10687

Fig. 5 Relationship between the rotational-vibrational line of NO and the Zeeman split atomic line.

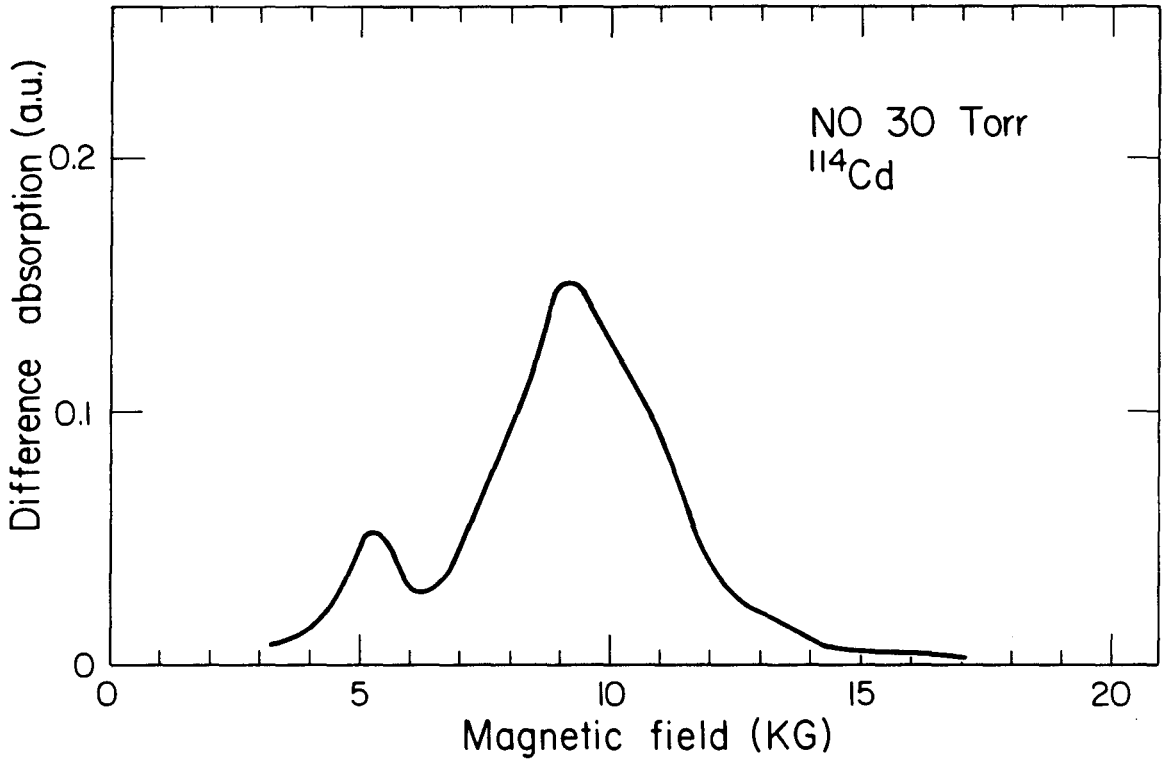

XBL 795-1605

Fig. 6 Relation between the magnetic field strength and the differential absorption caused by NO for the Cd(II) line at 214.4 nm.

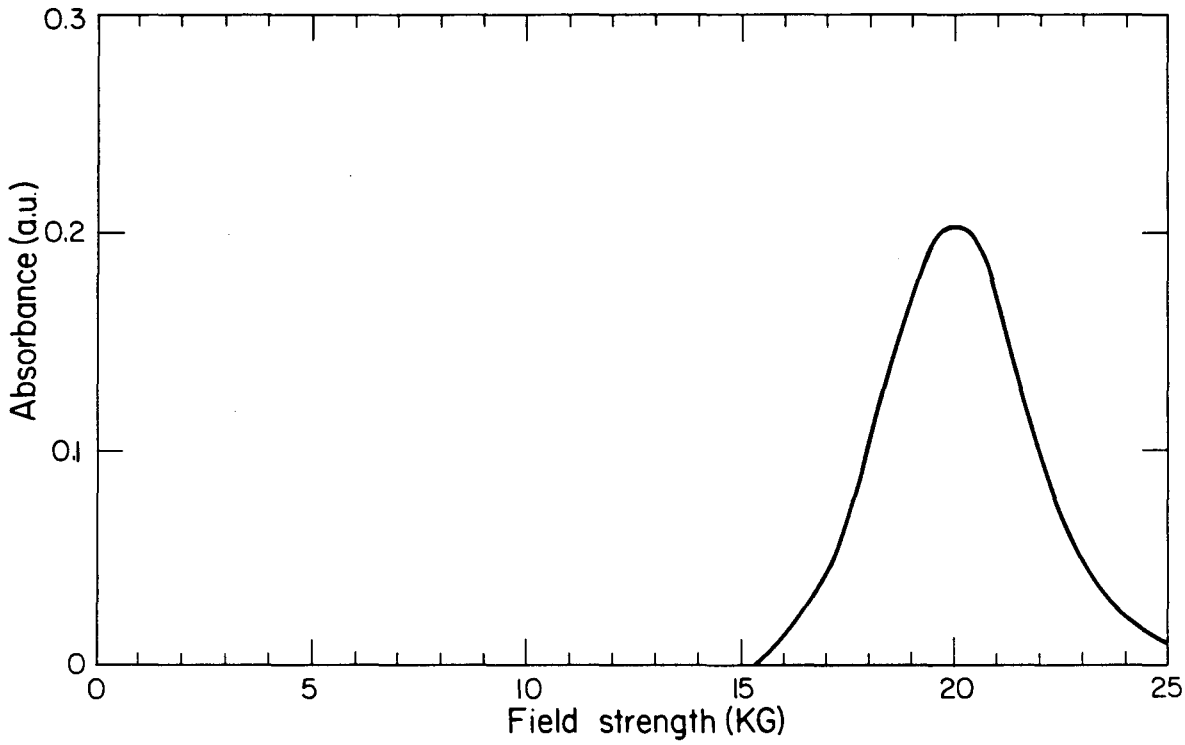

Fig. 7 Relation between the field strength and the differential absorption caused by NO for the Zn line at 213.9 nm.

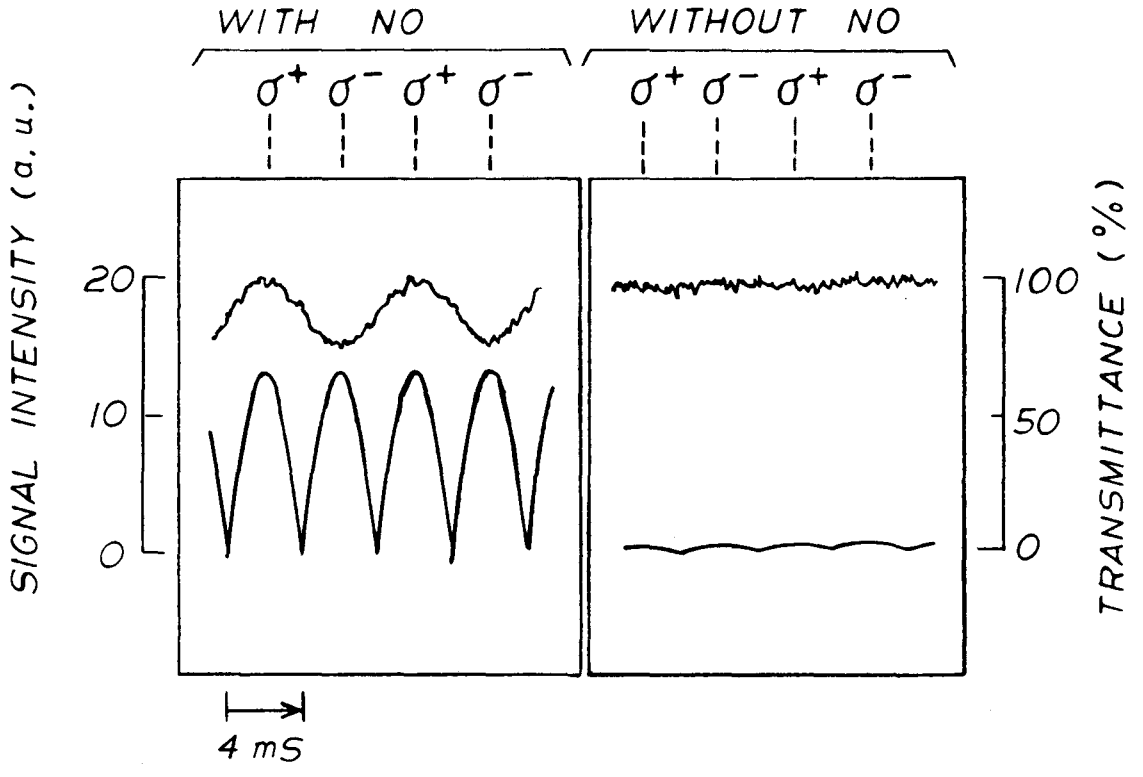

Fig. 8 Oscilloscope traces of the signal from the photomultiplier and from the synchronous rectifier.

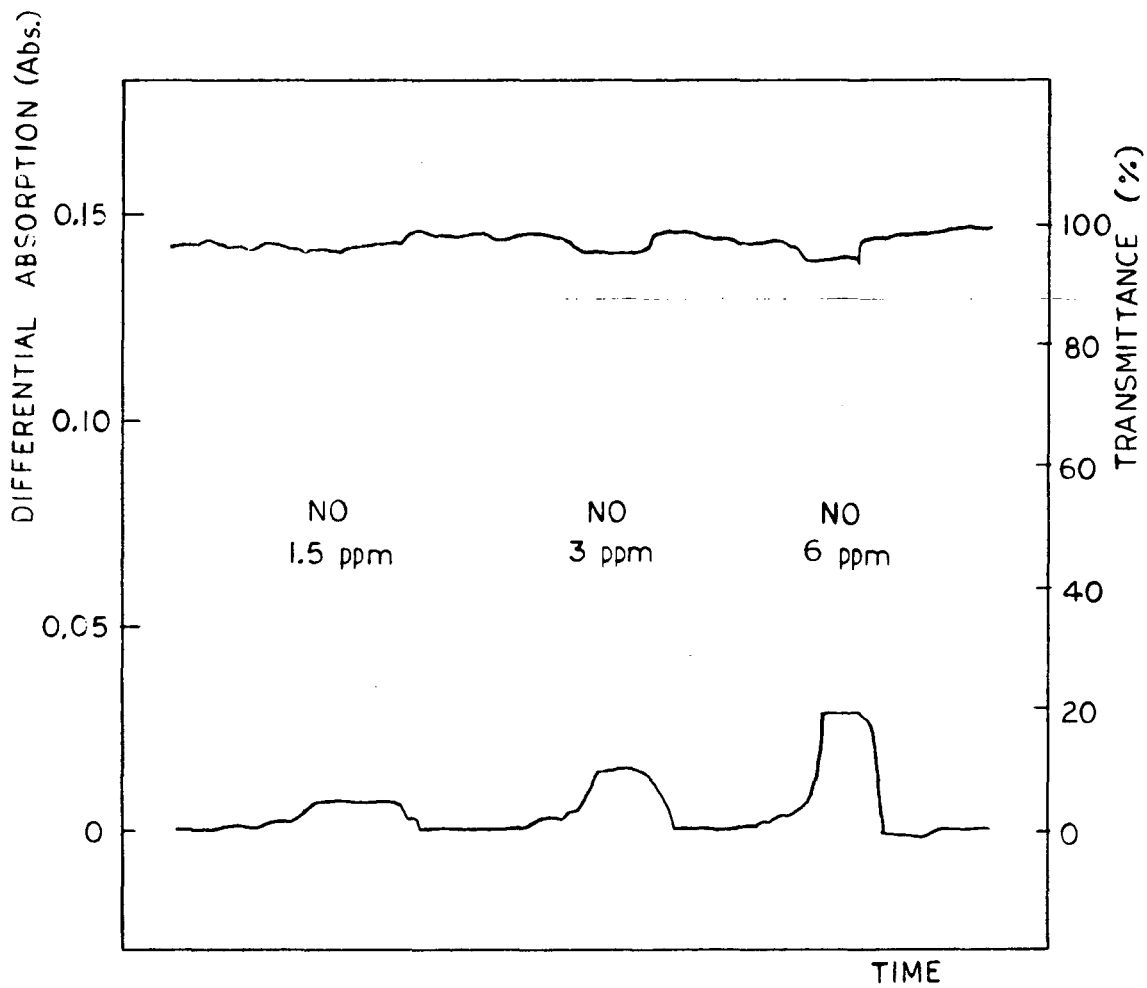

Fig. 9 NO signal with the present technique,

lower trace: differential signal.

upper trace: transmittance of light through the cell.

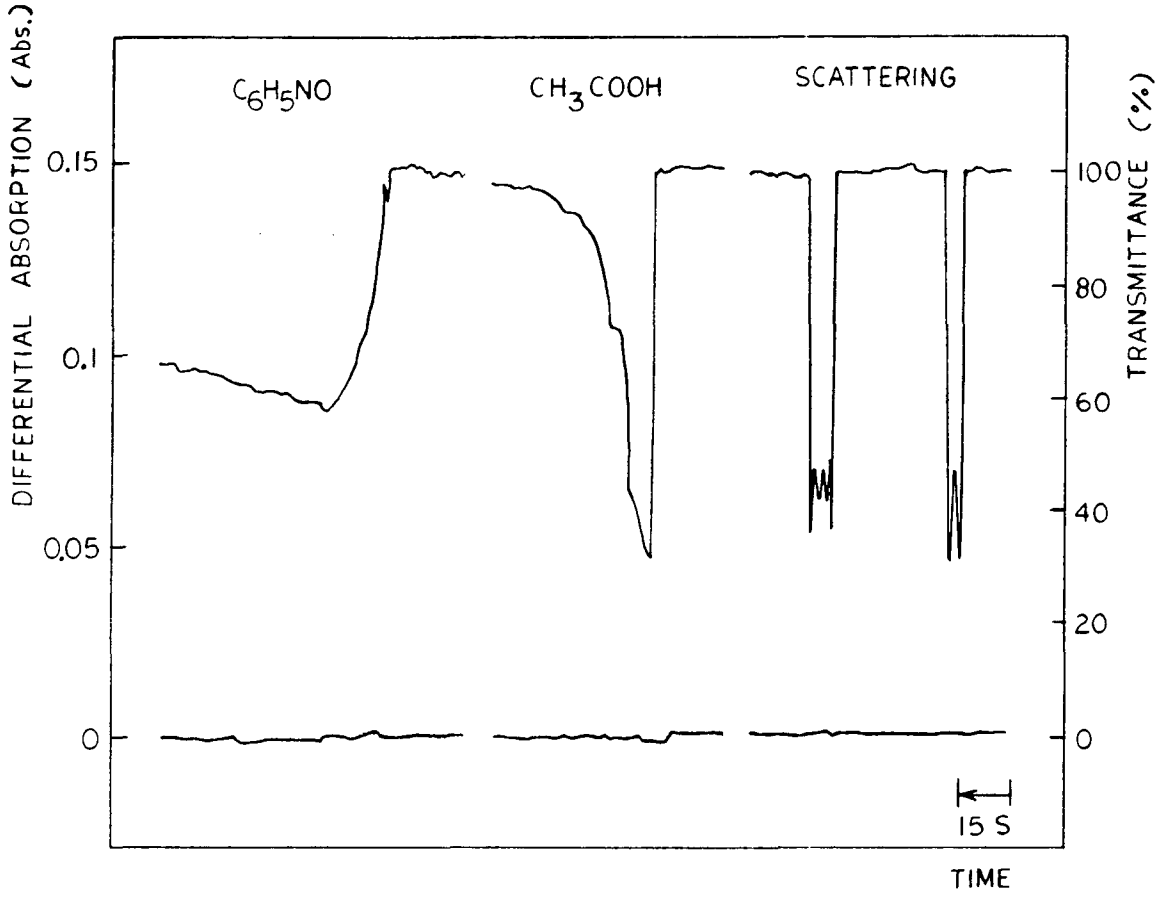

XBL 789-10677

Fig. 10 Correction for light scattering and absorption by other molecules,
lower trace: differential signal
upper trace: transmission through the cell in absorbance unit.

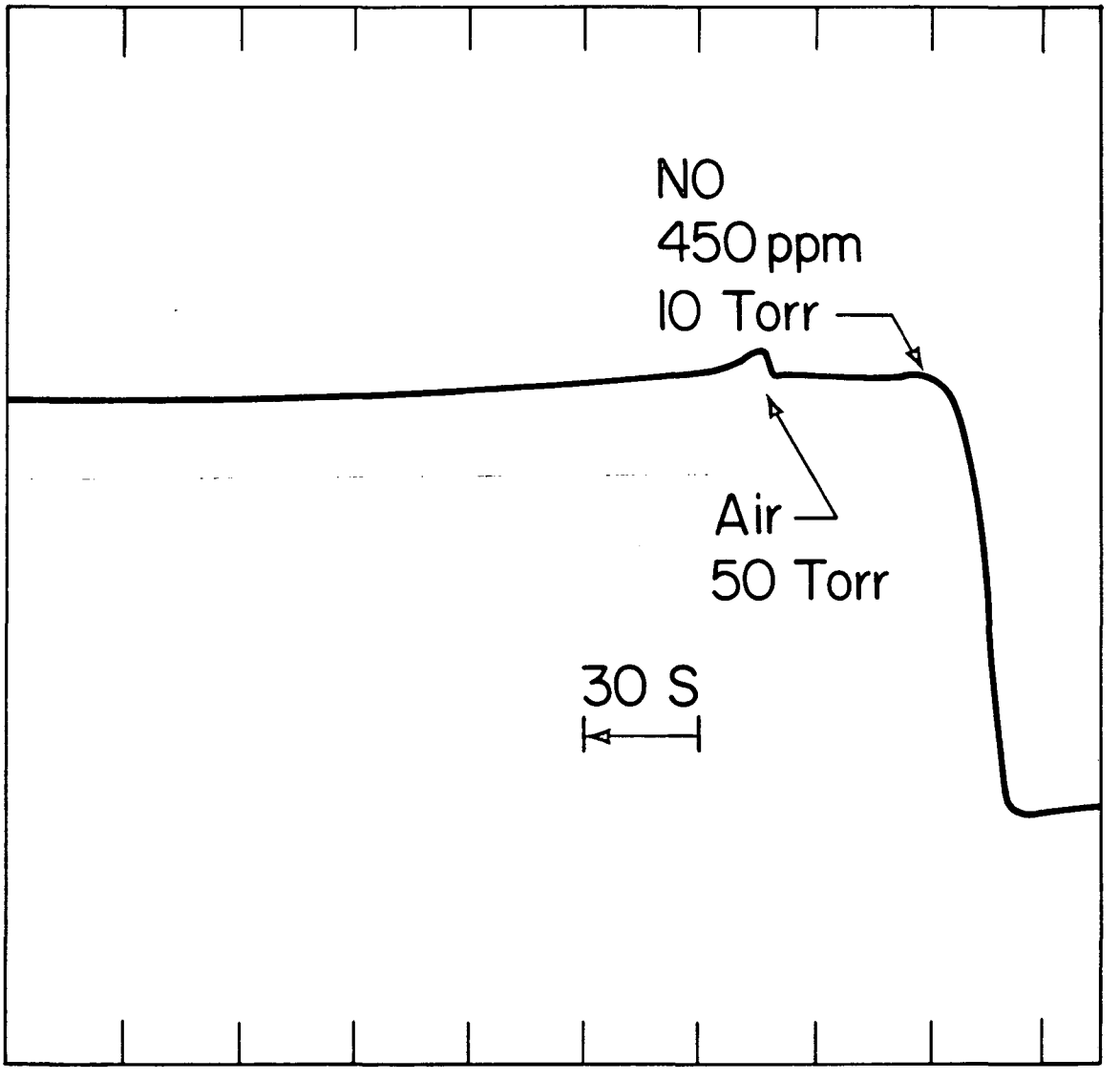

XBL 795-1609

Fig. 11 Time dependent NO signal after the introduction of air.

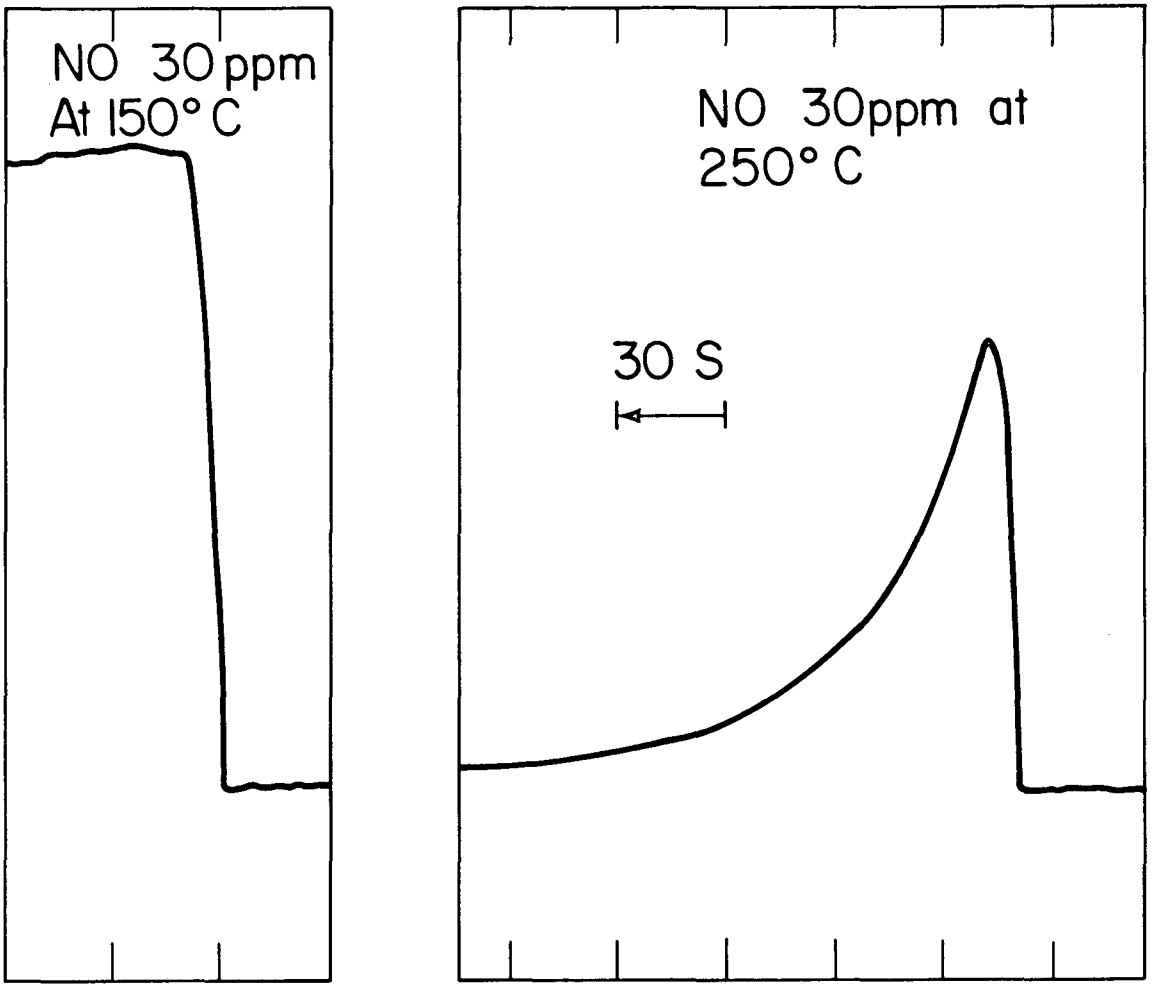

XBL 795-1610

Fig. 12 Reduction of NO signal because of reaction with the walls of a stainless steel cell at high temperature.

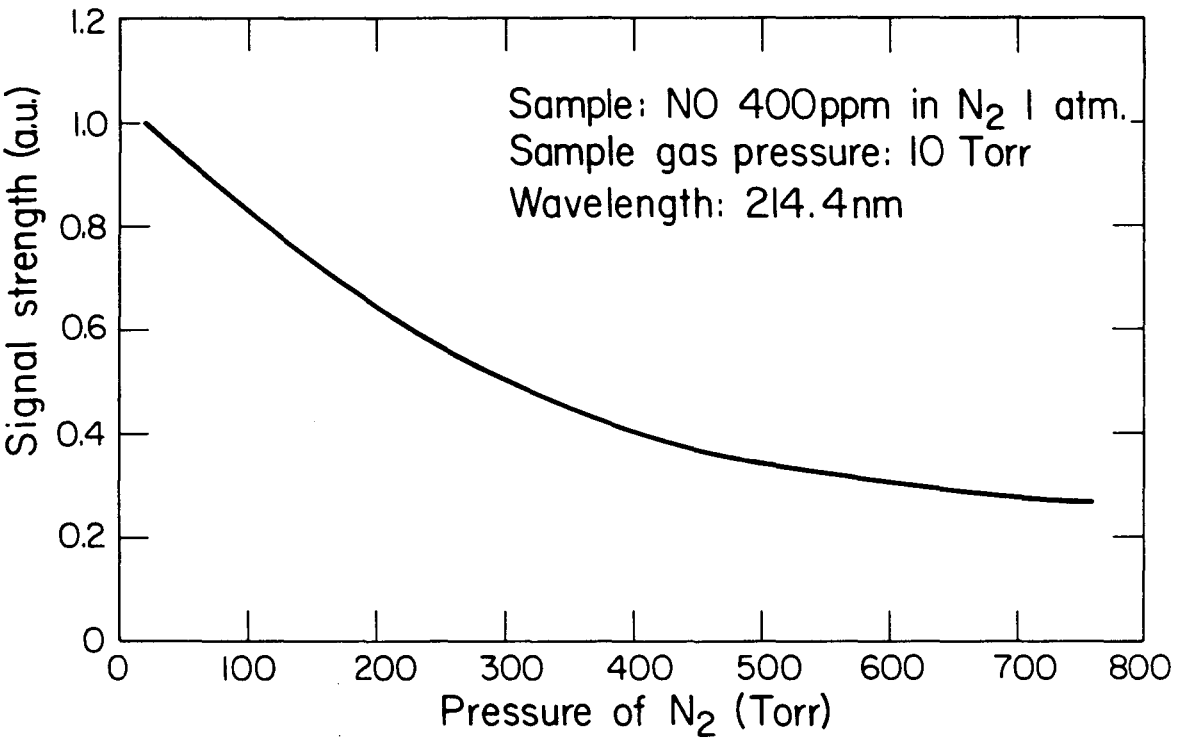

XBL 795-1608

Fig. 13 Relation between the differential absorption signal of NO and the pressure of the coexisting N_2 gas.

TECHNICAL INFORMATION DEPARTMENT
LAWRENCE BERKELEY LABORATORY
UNIVERSITY OF CALIFORNIA
BERKELEY, CALIFORNIA 94720